

Photoemission studies of CuInSe₂ and CuGaSe₂ and of their interfaces with Si and Ge

M. Turowski,* G. Margaritondo,[†] and M. K. Kelly

Department of Physics, University of Wisconsin, Madison, Wisconsin 53706

R. D. Tomlinson

Department of Electronics and Electrical Engineering, University of Salford, Salford M5 4WT, United Kingdom

(Received 4 June 1984)

We studied the electronic structure of two fundamental components of the $A^I B^{III} X_2^{VI}$ family of semiconductors by synchrotron-radiation photoemission. The experiments investigated the clean-surface density of occupied states, the Cu d -band satellites with photoemission resonant behavior at the Cu $3p$ optical absorption threshold, and the absolute energy position of the valence-band edges, E_v . In particular, we estimated the E_v terms (relative to the top of the valence band of Ge), which can be used to determine the band discontinuities of heterojunctions involving these materials. As an example, the E_v term obtained for CuInSe₂ was used to predict the conduction-band discontinuity of the CuInSe₂/CdS heterojunction solar cell.

I. INTRODUCTION

We present and discuss the result of a synchrotron-radiation photoemission study of CuInSe₂ and CuGaSe₂. These materials and in general the $A^I B^{III} X_2^{VI}$ chalcopyrite semiconductors have attracted much attention in the past several years.¹⁻⁸ They have potentially interesting applications in photovoltaic solar cells,^{1,2} light-emitting diodes,³ and various nonlinear devices.⁴ Their physical properties were the subject of many experimental and theoretical investigations.^{4-6,8} In particular, their theoretical electronic structure was extensively studied by Jaffe and Zunger.⁸ The experimental data on the electronic structure, on the other hand, is still limited.^{9,10} This is particularly true for the "absolute" position of the band edges which can be used to estimate the band discontinuities of heterojunction devices.¹¹

The present paper eliminates important gaps in our knowledge of the electronic properties of CuInSe₂ and CuGaSe₂, completing the preliminary work described in Ref. 12. Photoemission spectra were taken on clean surfaces obtained by fracturing under ultrahigh vacuum conditions, and used as a reference for the subsequent experiments. In particular, we observed for the clean surfaces resonant photoemission phenomena characteristic of Cu and of its compounds.^{13,14} Then we studied the formation of the CuInSe₂/Ge, CuInSe₂/Si, and CuGaSe₂/Ge interfaces. Photoemission spectra taken at different stages of the interface-formation process were used to estimate the valence-band discontinuity following the approach described, for example, in Ref. 15. From these results we deduced the absolute valence-band-edge-position terms for the two compounds.^{11,15} Combined with other terms in the Katnani-Margaritondo table,¹¹ these parameters can be used for a first-order estimate of the valence-band discontinuities of technologically important heterojunction devices. We were able, for example, to estimate the CuInSe₂/CdS valence-band discontinuity, obtaining a value in excellent agreement with transport results and in

general with the solar-cell performances of the device.^{1,7}

Section II of this paper gives a brief description of the experimental procedure and describes the clean-surface results. Section III discusses the results of the interface-formation processes, and Sec. IV summarizes our conclusions.

II. EXPERIMENTAL PROCEDURE AND CLEAN-SURFACE RESULTS

The experiments were performed at the "Grasshopper Mark II" beam line of the University of Wisconsin Synchrotron Radiation Center, using the instrumentation and the procedure described in Refs. 11 and 15. The essential parameters of the experiments were photon energy range 60–120 eV corresponding to an overall resolution (monochromator plus cylindrical mirror electron energy analyzer) of 0.3–0.6 eV and working pressure in the low 10^{-10} Torr range including the overlayer-deposition procedures. The single-crystal samples were grown at the University of Salford using the vertical Bridgman method for n -type CuInSe₂ and the horizontal-zone-growth process for CuGaSe₂.¹⁶ They were cut, etched with 1 vol. % Br-methanol, and mounted on Cu samples holders with vacuum-compatible epoxy and conducting glue. Clean surfaces were obtained under ultrahigh vacuum by fracturing the samples *in situ* with a tungsten blade. Clean-surface photoemission spectra of the valence band and of the In $4d$, Ga $3d$, Cu $3p$, and Se $3d$ were taken at photon energies selected to enhance the surface sensitivity of the photoemission probe by minimizing the photoelectron escape depth.

Thin overlayers of Ge were obtained by evaporation from a tungsten basket monitored with a quartz-crystal oscillator. Silicon was deposited instead by bombardment with 4.5-keV electrons. Photoemission spectra were taken at each stage of coverage for the above features and for the Ge $3d$ and Si $2p$ core levels. Spectra taken before and after overlayer deposition revealed no contamination. We

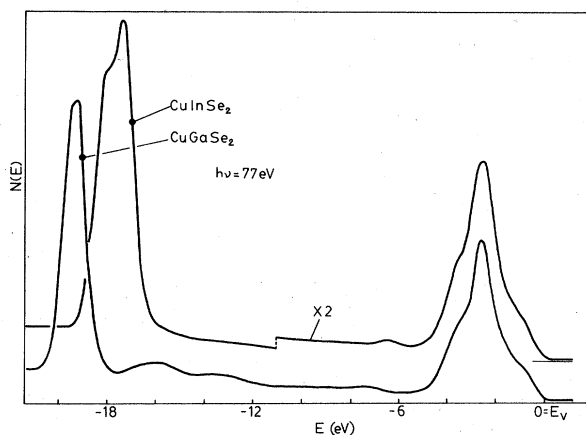


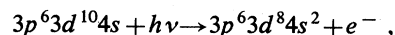
FIG. 1. Photoelectron energy distribution curves (EDC's) taken on clean CuInSe₂ and CuGaSe₂ surfaces at $h\nu=77$ eV. The zero of the energy scale is the top of the valence band, E_v .

estimate, in particular, the contamination by oxygen, carbon, and their compounds to be less than $\frac{1}{100}$ monolayer.

Figure 1 shows valence-band photoemission spectra taken on clean CuInSe₂ and CuGaSe₂. These results were used to test the quality of our substrates by comparing them with previous data by Rife *et al.*⁹ for CuInSe₂ and by Braun and Lannin¹⁰ for CuGaSe₂, and with the theoretical predictions of Jaffe and Zunger.⁸ Table I summarizes the results of this comparison and demonstrates that there is a reasonable qualitative and quantitative correspondence between the different sets of values. The quantitative discrepancies between our binding energies and those of Ref. 9 are due in part to a different estimate of the valence-band-edge position—the band-edge signal is stronger in our spectra than in the x-ray photoemission spectra of Ref. 9. The largest discrepancies affecting the Cu 3*d* features are probably due to transition probability modulation, which also explains the differences in line shape between our valence-band spectra and those of Ref. 9.

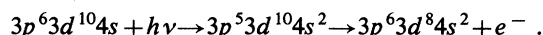
The clean-surface spectra of Fig. 1 are dominated by the Cu 3*d* features and by their satellites. The satellite structure is particularly prominent in the CuGaSe₂ spectra and it consists of two peaks ~ 11 and 13.5 eV below the

estimated center of the *d* band. Similar satellite structure have been observed for metallic Cu (Ref. 13) and for quasi-matrix-isolated Cu in Cu-phtalocyanine.¹⁴ The mechanism proposed to explain it is a shake-up process that leaves two holes in the Cu *d* band:



and the two-peak structure is characteristic of the 3*d*⁸ configuration. The energy separation between the satellite peaks and the center of the *d* band is 2.5–3 eV larger for our samples than for metallic Cu.¹³ Likewise, the separation increases¹⁴ on going from quasi-matrix-isolated or atomic Cu to metallic Cu. Iwan *et al.*¹⁴ attributed that effect primarily to the larger screening of the 3*d*⁹ one-hole state. The same explanation cannot be extended to our materials, for which the screening brings the 3*d*⁹ initial energy to a value intermediate between quasi-matrix-isolated and metallic Cu. Therefore, the different separation between satellites and *d* band must be attributed to differences in the configuration (and possibly screening) shifts of the 3*d*⁸ two-hole state between metal Cu and our samples.

One interesting property of the Cu satellite is their resonant photoemission behavior at photon energies corresponding to the Cu 3*p* optical-absorption threshold.^{13,14} Similar resonances were observed for the well-known Ni satellite,¹⁷ but the explanations typically proposed for that phenomenon cannot be extended to Cu which has filled *d* bands. The proposed explanation for Cu (Ref. 13) is the Fano interference between the above shake-up process and the following excitation-Auger process leading to the same final state:



The effects of the resonant enhancement were clearly visible for our materials. Figure 2, for example, shows the resonant behavior of the *d*-band satellite in CuGaSe₂ at the threshold energy $h\nu=77$ eV. At resonance the intensity of the satellite peaks increases by about a factor of 3. The resonant behavior removes the doubts about the nature of the shallowest satellite peak, which might have been caused by the coincidence of its position with the calculated X^{VI} band.⁸ In principle, additional information on the nature of the satellites could be obtained from

TABLE I. Calculated and experimental binding energies of the clean-surface photoemission features of CuInSe₂ and CuGaSe₂. Binding energies in eV, relative to the top of the valence band, E_v . The theoretical values are from Ref. 8.

Feature	CuInSe ₂		CuGaSe ₂			
	Theory	Ref. 9	This work	Theory	Ref. 10	This work
Cu 3 <i>d</i>	3.3	0.5	1.0	3.2	1.0	1.0
Cu 3 <i>d</i>	4.2	2.1	2.7	4.1	2.4	2.7
$B^{III}-X^{VI}$ band	6.0	3.3	3.7	6.6	3.5	3.6
X^{VI} band and	13.0	6.3	6.5	13.2	7.0	7.35
Cu satellites ^a		13.0	13.2			13.5, 16.0
B^{III} <i>d</i> core level	16.9	17.5	17.65	17.5		19.35

^aThe resonant behavior of these peaks indicates that they are Cu *d*-band satellites rather than the X^{VI} band features theoretically predicted (Ref. 8) at the same energy (see text).

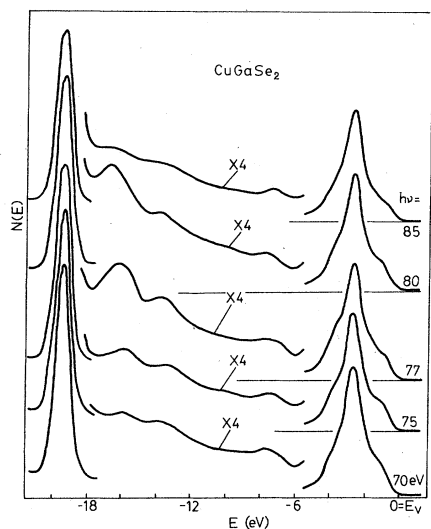


FIG. 2. CuGaSe_2 EDC's taken at different photon energies reveal the resonant photoemission cross section of the Cu d -band satellites 13.5 and 16.0 eV below E_v at photon energies close to the Cu $3p$ optical-absorption threshold.

the detailed Fano line shape of their intensity versus $h\nu$ plots. These plots, however, are affected by the underlying nonresonant Auger emission in the same kinetic-energy range.¹⁸ A reliable correction method was recently proposed by Riedel *et al.*,¹⁸ but it could not be applied to our spectra due to the proximity of the intense $B^{\text{III}} d$ core-level emission.

III. RESULTS ON Si AND Ge CHEMISORPTION

A detailed knowledge of the electronic structure is an essential prerequisite for the understanding of the physical properties of semiconducting materials and ultimately for their practical use in solid-state devices. Spectra such as those of Figs. 1 and 2 are an important source of information about the electronic states. The importance of other pieces of information has been emphasized in recent years by extensive research on semiconductor interfaces. Some of the most interesting applications of the materials discussed here are in the area of heterojunction devices.^{1,7} Photoemission measurements of the *absolute* position in energy of the band edges are of immediate interest in the physics of heterojunctions. In fact, Katnani and Margaritondo¹⁵ empirically demonstrated that those positions are the most important factor in determining the heterojunction band discontinuities. In turn, the band discontinuities play the most important role in the transport properties of heterojunction devices.

The existence of a valence-band discontinuity ΔE_v and of a conduction-band discontinuity ΔE_c at the interface between two semiconductor is due to the difference between the two forbidden gaps. In principle, ΔE_v and ΔE_c can be influenced by several microscopic factors which determine the local charge distribution and in particular the interface dipoles. These factors, however, do not contribute by more than 0.1–0.2 eV to the discontinuities.¹⁵

Nonlocal factors, i.e., the absolute energy positions of the electronic states of the two semiconductors, are the most important factors contributing to ΔE_v and ΔE_c .¹⁵ The experimental evidence for this elementary fact explains why very simple, nonlocal theories are able to predict the discontinuities with remarkably good accuracy.^{11,15,19–23} In the best case^{11,19,20} nonlocal theories reach the 0.1–0.2-eV accuracy limit due to the local contributions to ΔE_v and ΔE_c they neglect. This is still insufficient for practical applications, but quite good if one considers the approximate character of these approaches. No current theory, in practice, is able to overcome the 0.1–0.2-eV accuracy limit.¹⁵

An optimized empirical version of the nonlocal approaches to estimate the discontinuities was proposed in Ref. 11. It consists of determining for each semiconductor the absolute position of the valence-band edge, E_v , and then of estimating ΔE_v for each pair of semiconductors by taking the difference of the corresponding E_v terms. E_v terms were empirically deduced^{11,15} for each material from photoemission spectra taken during the formation of interfaces between that material and a reference semiconductor, Ge or Si. Reference 15 deduced the E_v terms for the most important elemental and binary semiconductors. We extend here the same approach to materials in the $A^{\text{I}}B^{\text{III}}X_2^{\text{VI}}$ family.

Following Ref. 15, we referred the E_v 's to the top of the valence band of Ge. Therefore, the E_v terms were determined by measuring the discontinuity ΔE_v for the interface between each material and Ge—or Si, after correcting for the known discontinuity between Si and Ge.¹⁵ Figure 3 shows the evolution of the leading edge of the photoemission spectra during progressive coverage of CuInSe_2 by Ge. The position of E_v for each coverage is estimated from the linear extrapolation of the leading edge. E_v shifts by 0.32 eV on going from clean CuInSe_2

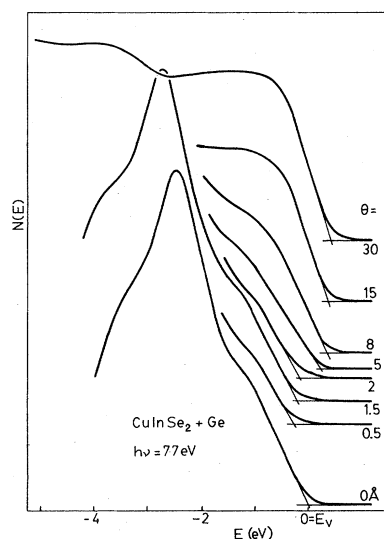


FIG. 3. Evolution of the leading EDC edge for Ge-covered CuInSe_2 as a function of the Ge coverage, Θ . The zero of the energy scale is the top of the clean-surface CuInSe_2 valence band.

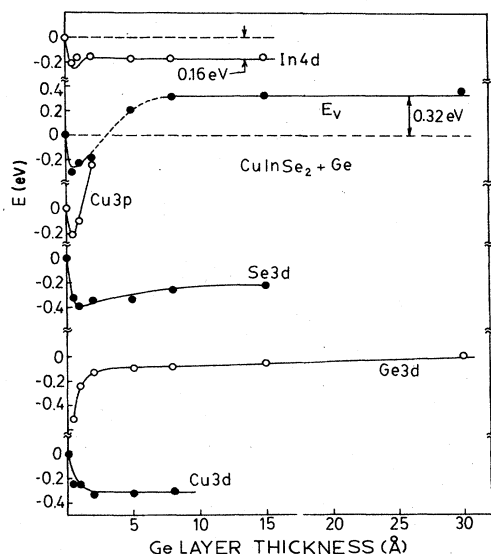


FIG. 4. Energy shifts of the $\text{CuInSe}_2/\text{Ge}$ photoemission spectral features as a function of the Ge overlayer thickness. Scale is relative to the clean-surface CuInSe_2 valence-band edge. The shift of each feature was relative to the clean-surface position except for the Ge 3d peak which was relative to the large-coverage position.

to the 30-Å spectrum which is already representative of bulk Ge. This shift does *not* directly correspond to the valence-band discontinuity ΔE_v between CuInSe_2 and Ge, since the position of the substrate valence-band edge at the interface is modified by adatom-induced changes in the band bending. To obtain ΔE_v , therefore, we need an independent estimate of the band-bending changes.

In principle, the estimate can be obtained by monitoring the corresponding shifts of the substrate core-level photoemission peaks. These shifts, however, can be also influenced by changes in the chemical shift. A deconvolution of the two contributions is not an easy task, and it requires a careful analysis of several core-level and valence-band spectral features.¹⁵ Figure 4 shows the positions in energy of E_v , of the peak of the Cu d band and of the In 4d, Cu 3p, and Se 3d peaks for CuInSe_2 as a function of Ge coverage. The first three features were deduced from $h\nu=77\text{-eV}$ spectra and the last two features from $h\nu=90\text{-eV}$ spectra. For most binary semiconductors we found¹⁵ that the anion core levels are heavily affected by adatom-induced changes in the chemical shift, and therefore they cannot be used to estimate band-bending changes. In fact, we see in Fig. 4 that for coverages up to 2 Å the Se 3d shift is much larger than the shift of E_v —which for low coverages is primarily due to band-bending changes. We also found¹⁵ that for most binary semiconductors the cation peaks are not affected by changes in the chemical shift, and therefore their adatom-induced shifts can be directly used to estimate the changes in band bending. This rule cannot be immediately applied to our materials due to the presence of two different cation species. The line shape changes of the Cu d band and the shift of the Cu 3p peak indicate that Cu atoms are involved in the

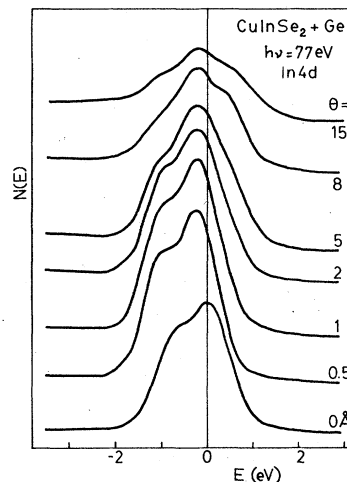


FIG. 5. Evolution of the In 4d peak during the formation of the $\text{CuInSe}_2/\text{Ge}$ interface. The energy scale is relative to the position of the In $4d_{5/2}$ component for clean CuInSe_2 . Notice the line shape of the large-coverage spectra which is due to the presence of two different In 4d doublets. The shift in energy of the left-hand-side doublet reflects the adatom-induced changes in the substrate band bending (see text).

formation of interface chemical bonds—and therefore that the Cu features are affected by adatom-induced changes in their chemical shift and cannot be directly used to estimate the band-bending changes. Figure 5 shows that the line shape of the In 3d peak also changes during the formation of the interface. At large coverages there is evidence for two components, shifted by ~ 0.7 eV with respect to each other. The highest in energy of the two components can be attributed to presence of free In released from the substrate during the interface-formation process. The deepest component is the substrate In 4d peak, whose position is determined by the substrate band bending. The In 4d shift shown in Fig. 4 is that of this substrate component. The correspondence between its shift and the band-bending changes is confirmed by the low-coverage similarity with the shift of E_v .

The total band-bending change estimated from the shift of the substrate In 4d peak is -0.16 eV. Combined with the total shift of E_v , this value gives $\Delta E_v = 0.32 - (-0.16) = 0.48$ eV for the $\text{CuInSe}_2/\text{Ge}$ interface. Similar experiments were performed for the $\text{CuInSe}_2/\text{Si}$ interface, and a preliminary description was given in Ref. 12. The analysis was simplified by the absence of the free-In component in the In 4d peak, whose position directly reflected the substrate band bending. The total band-bending change for $\text{CuInSe}_2/\text{Si}$ was 0.38 eV and the E_v shift was also 0.38 eV, giving $\Delta E_v = 0.00$ eV.

The difference between the values of ΔE_v for $\text{CuInSe}_2/\text{Ge}$ and $\text{CuInSe}_2/\text{Si}$ is in qualitative agreement with the fact that the E_v term for Si (relative to the top of the valence band of Ge) is negative.¹⁵ Quantitatively, however, there is a substantial discrepancy between the difference, -0.48 eV, and the Si E_v term, -0.17 eV.

This discrepancy is larger than the experimental uncertainty, which can be estimated¹⁵ not to exceed ± 0.1 eV, and larger than the typical discrepancies found for other substrates, 0.1–0.2 eV. This indicates that the interface dipoles contributing to ΔE_v are markedly different for Si and Ge overlayers. This conclusion is consistent with the different microscopic structure of the interface, suggested, for example, by the presence of a free-In 4*d* component for CuInSe₂/Ge which is not observed for CuInSe₂/Si.¹²

The E_v term for CuInSe₂, relative to the top of the valence band of Ge, was estimated by taking the average of the ΔE_v for CuInSe₂ and of the ΔE_v for CuInSe₂/Si corrected for the Si E_v term.¹⁵ The result is $[-0.48 + (0.00 - 0.17)]/2 = -0.32$ eV, where the minus sign means that the top of the valence band of CuInSe₂ is below that of Ge. Due to the above discrepancy between the ΔE_v 's for Si and Ge overlayers, the estimated accuracy of this term is ± 0.15 eV, i.e., slightly worse than that of the other terms of the Katnani-Margaritondo table.¹¹ An immediate application of the deduced ΔE_v terms is the explanation of the good efficiency of (*p*-type CuInSe₂)/(*n*-type CdS) heterojunction solar cells.^{1,7} It was proposed that the most crucial factor in determining the performances of those devices is the absence of an interface "spike" in the conduction band.^{1,7} This hypothesis can be directly tested with our results. The E_v term for CdS is -1.73 eV. Combined with the E_v term for CuInSe₂, this gives an estimated valence-band discontinuity $\Delta E_v = 1.41$ eV for CuInSe₂/CdS (i.e., with the CuInSe₂ E_v above that of CdS). The gap difference between CdS and CuInSe₂ is $2.42 - 1.04 = 1.38$ eV. Therefore, the estimated conduction-band discontinuity for

CuInSe₂/CdS is $\Delta E_c = 1.38 - 1.41 = -0.03$ eV. This is consistent with the absence of an interface spike in the conduction band.

Transport measurements⁷ give ΔE_c values of -0.07 and -0.08 eV for CuInSe₂/CdS,¹² in excellent agreement with our estimate. Neither our accuracy nor that of transport measurements is sufficient to distinguish the above values from a perfectly flat conduction-band edge at the interface. However, the combination of all the estimates with their accuracies indicates that ΔE_c is in fact negative, i.e., that the conduction-band edge of CuInSe₂ is slightly above that of CdS. This is an interesting fact, since a negative ΔE_c helps separate the photoexcited electron-hole pairs in the (*p*-type CuInSe₂)/(*n*-type CdS) solar cell preventing recombination and increasing the efficiency, as schematically shown in Fig. 6. Also shown in Fig. 6 is a summary of the band lineup results for the materials here investigated and for CdS.

We extended our interface-formation studies to the CuGaSe₂/Ge system. Figure 7 shows the shifts of the photoemission features of this system as a function of Ge coverage. The Ga 3*d* peak did not provide evidence for two different chemical environments of the Ga atoms at large Ge coverages, in contrast to the results for the In 4*d* peaks in CuInSe₂/Ge. Once again we see in Fig. 7 that neither the anion core-level peak nor the Cu features exhibit shifts similar to that of E_v at low Ge coverages—i.e., those shifts do not directly reflect the changes in band bending. The initial shift of the Ga 3*d* peak, instead, is similar to that of E_v . We conclude that, similar to the In 4*d* peak in CuInSe₂/Ge and CuInSe₂/Si, the Ga 3*d* peak can be used to monitor the changes in substrate band bending. In fact, its behavior indicates that after some initial changes the final band bending is equal to that of the clean CuGaSe₂ surface. Therefore, the total shift of E_v coincides with the valence-band discontinuity, $\Delta E_v = 0.62$ eV. This value is larger than the value for CuInSe₂/Ge (and its E_v term relative to the top of the valence band of

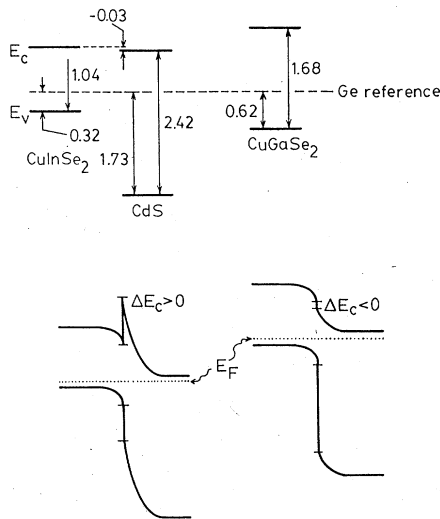


FIG. 6. Top: summary of the band lineup results for the semiconductors here investigated and for CdS (energies in eV). Bottom: Qualitative band diagrams of a (*p*-type CuInSe₂)/(*n*-type CdS) heterojunction solar cell for positive and negative ΔE_c 's. A positive ΔE_c would introduce a spike in the conduction-band edge, which would prevent the separation of the photogenerated electrons from the photogenerated holes. This would decrease the efficiency of the cell. The experimental results, however, indicate that $\Delta E_c < 0$ and that the spike does not exist.

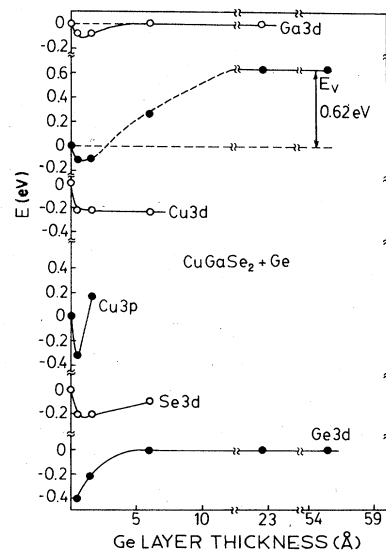


FIG. 7. Energy shifts of the CuGaSe₂/Ge spectral features during the interface-formation process.

Ge). A similar trend was observed¹⁵ for binary In and Ga compounds with the same anion.

IV. CONCLUSIONS

We studied the electronic structure of two fundamental materials in the $A^I B^III X_2^{VI}$ family, CuInSe₂ and CuGaSe₂, by synchrotron-radiation photoemission. We found that the Cu *d*-band satellite peaks already observed for metal Cu and for matrix-isolated Cu are also visible in these compounds. They exhibit a resonant photoemission cross section at the Cu 3*p* absorption threshold, similar to that observed for Cu in other chemical environments. Experiments on the formation of interfaces between the two compounds and elemental semiconductors determined the

absolute energy positions of their valence-band edges. Relative to the top of the valence band of the Ge edge, we estimate E_v to be at -0.32 ± 0.15 eV for CuInSe₂, and at -0.62 ± 0.15 eV for CuGaSe₂. The E_v term for CuInSe₂ provides a direct explanation for the good efficiency of CuInSe₂/CdS solar cells, in agreement with transport measurements.

ACKNOWLEDGMENTS

This work was supported by the National Science Foundation (NSF), under Grant No. DMR-82-00518, and was made possible by the friendly and competent help of the entire staff of the NSF-supported University of Wisconsin Synchrotron Radiation Center, Stoughton.

*On leave from the Institute of Physics, Jagellonian University of Cracow, Poland.

† Author to whom all correspondence should be addressed.

¹S. Wagner, J. L. Shay, P. Migliorato, and H. M. Kasper, *Appl. Phys. Lett.* **25**, 434 (1974); J. L. Shay, S. Wagner, and H. M. Kasper, *ibid.* **27**, 89 (1975).

²R. A. Mickelsen and W. S. Chen, *Proceedings of the 16th IEEE Photovoltaic Specialists Conference* (IEEE, New York, 1982), p. 781.

³N. Yamamoto, *Jpn. J. Appl. Suppl.* **19-3**, 45 (1980).

⁴B. R. Pamplin, T. Kiyosawa, and K. Masumoto, *Prog. Cryst. Growth Charact.* **1**, 331 (1979).

⁵J. L. Shay and H. H. Wernic, *Ternary Chalcopyrite Semiconductors: Growth, Electronic Properties and Applications* (Pergamon, Oxford, 1975).

⁶A. Miller, A. MacKinnon, and D. Weaire, *Solid State Physics*, edited by H. Ehrenreich, F. Seitz, and D. Turnbull (Academic, New York, 1981), Vol. 36, p. 119.

⁷L. L. Kazmerski, J. P. Ireland, F. R. White, and R. B. Cooper, *Proceedings of the 13th IEEE Photovoltaic Specialists Conference* (IEEE, New York, 1978), p. 184.

⁸J. E. Jaffe and A. Zunger, *Phys. Rev. B* **28**, 5822 (1983).

⁹J. C. Rife, R. N. Dexter, P. M. Bridenbaugh, and B. W. Veal, *Phys. Rev. B* **16**, 4491 (1977).

¹⁰W. Braun and J. S. Lannin, *Proceedings of the 12th International Conference on the Physics of Semiconductors, Stuttgart, 1974*, edited by M. H. Pilkuhn (Teubner, Stuttgart 1974), p.

1308.

¹¹A. D. Katnani, and G. Margaritondo, *J. Appl. Phys.* **54**, 2522 (1983).

¹²M. Turowski, M. K. Kelly, G. Margaritondo, and R. D. Tomlinson, *Appl. Phys. Lett.* **44**, 768 (1984).

¹³M. Iwan, F. J. Himpfel, and D. E. Eastman, *Phys. Rev. Lett.* **43**, 1829 (1979).

¹⁴M. Iwan, E. E. Koch, T. C. Chiang, D. E. Eastman, and F. J. Himpfel, *Solid State Commun.* **34**, 57 (1980).

¹⁵A. D. Katnani and G. Margaritondo, *Phys. Rev. B* **28**, 1944 (1983).

¹⁶J. Parkes, R. D. Tomlinson, and M. J. Hampshire, *J. Cryst. Growth* **36**, 151 (1976); L. Mandel, R. D. Tomlinson, and M. J. Hampshire, *ibid.* **36**, 151 (1976).

¹⁷C. Guillot, Y. Ballu, J. Paigne, J. Lecante, K. P. Jain, P. Thiry, R. Pinchaux, Y. Petroff, and L. M. Falicov, *Phys. Rev. Lett.* **39**, 1632 (1977).

¹⁸R. A. Riedel, M. Turowski, G. Margaritondo, and P. Perfetti, *Phys. Rev. Lett.* **52**, 1568 (1984).

¹⁹W. Harrison, *J. Vac. Sci. Technol.* **14**, 1016 (1977).

²⁰W. R. Frensley and H. Kroemer, *Phys. Rev. B* **15**, 2642 (1977).

²¹R. L. Anderson, *Solid State Electron.* **5**, 341 (1962).

²²M. J. Adam and Allen Nussbaum, *Solid State Electron.* **22**, 783 (1979).

²³Oldwig Von Ross, *Solid State Electron.* **23**, 1069 (1980).